ACS OMEGA

http://pubs.acs.org/journal/acsodf

Article

Unconventional OFF−ON Response of a Mono(calix[4]arene)-Substituted BODIPY Sensor for Hg^{2+} through Dimerization Reversion

Alejandro Lorente,* Andres Ochoa, Julio Rodriguez-Lavado, Silvia Rodriguez-Nuévalos, Pablo Jaque,* Salvador Gil, José A. Sáez,* and Ana M. Costero

Cite This: *ACS Omega* 2023, 8, 819−828

Read Online

ACCESS | Metrics & More | Article Recommendations | Supporting Information

ABSTRACT: A new selective fluorogenic chemosensor for Hg^{2+}, which combines a calixarene derivative with a BODIPY core as a fluorescent reporter, is described. The remarkable change in its fluorogenic properties in DMSO and $CHCl_3$ has been analyzed. A study of its spectral properties on dilution, along with molecular modeling studies, allowed us to explain that this behavior involves the formation of a J-dimer, as well as how the sensing mechanism of Hg^{2+} proceeds.

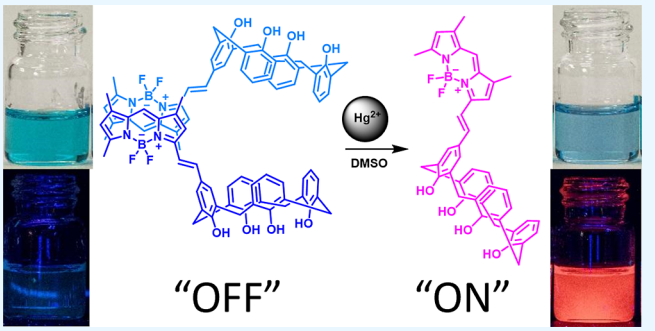

1. INTRODUCTION

Heavy metals play an essential role in our society. They are present in almost any application developed since the discovery of metallurgy. They are useful due to their intrinsic properties such as malleability, ductility, and thermal and electrical conductivity. Nevertheless, most of these metals can cause serious diseases if their concentrations in our bodies reach a certain level.[1] Such a situation has been occurring, for example, due to the uncontrolled disposal of heavy metal-containing wastes (e.g., from electronic devices or ore extraction and processing) rich in lead, mercury, arsenic, cadmium, chromium, copper, nickel, or zinc.[2,3] These metals can reach us by inhaling volatiles and dust, absorbing through the skin, or eating food grown in contaminated soil or water. In particular, mercury is extremely toxic and causes damage to the nervous, digestive, and immunologic systems, as well as the lungs, kidneys, skin, and eyes, among other organs.[4,5] Upon reaching the environment, mercury is transformed into its divalent salts (e.g., mercury chloride, methylmercury), which later bioaccumulate in fish and crustaceans, entering the food chain. Therefore, it is of high interest to dispose of techniques that allow the fast determination of Hg^{2+} in potentially polluted sources.

There exist several methods for the detection of these contaminants in the environment based on analytical techniques such as gas chromatography−mass spectroscopy, atomic absorption spectroscopy, and X-ray or laser-induced breakdown spectrometry.[6] Unfortunately, these methods are generally expensive and not portable, requiring long measuring times, significant amounts of samples, and qualified personnel. Alternatively, absorbance- and emission-based methods are becoming predominant because they are simpler to implement and also offer high sensitivity and specificity. Chemosensors have also been shown to be portable, easy to apply, and low-cost devices that are able to detect dangerous gases.[7]

In order to design suitable probes for metal detection, two main features have to be combined. On one side is a sensing unit, which can convert the recognition event of an analyte into an optical signal due to the perturbation of its photophysical properties.[8,9] Among the heterogeneous library of chromo- and fluorophores available in the literature,[10] 1,3,5,7-tetramethyl-4,4-difluoroboradiazaindacene (BODIPY) dyes have been gaining much attention since the late 1980s.[11,12] This is mainly due to their associated photophysical parameters, such as high stability, versatile chemical modification, and tunable emission and absorption properties,[13] which render them very attractive units for chemosensor development.[14−16] On the other side, a suitable receptor has to be connected to the fluorophore to form a supramolecular complex with the targeted metal cations. Within the many possible complexing ligands described,[17,18] calix[*n*]arenes have been of much interest in supramolecular chemistry, mainly because of their

Received: September 23, 2022
Accepted: December 5, 2022
Published: December 23, 2022

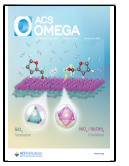

intrinsic selectivity and the possibility to modify their activated positions by incorporating them as a part of specific fluorophores.[19−22] Chemosensors combining calix[4]arene at the *meso*-position of the BODIPY core have been previously described as pH sensors[23] or for selective Ca^{2+} complexation.[24] Additionally, successful probes have been reported for exploiting the functionalization of calix[4]arene in its lower rim with triazoles[15] or thioureas,[25] which selectively coordinate with Hg^{2+}.

In this work, we aim to report a new chemosensor (**1**) to detect Hg^{2+} based on a BODIPY signaling unit and a calix[4]arene binding moiety (Chart 1). In addition to the sensing properties, the probe shows interesting fluorogenic properties compatible with dimer formation that are also discussed. Despite the fact that BODIPY-based molecules are well recognized as highly stable, mainly due to the nonpolar nature of their core, they tend to form aggregates in highly polar solvents (for instance, DMSO)[26] and are stabilized by $\pi-\pi$ stacking intermolecular interactions among others. These interactions are known for strongly altering the luminescence response mode and, consequently, the chemical sensing mechanism.

Chart 1. Probe for Hg^{2+} Sensing

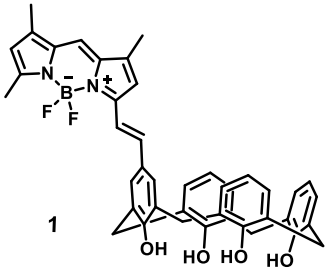

2. RESULTS AND DISCUSSION

2.1. Materials Design and Synthesis. BODIPYs are known to be easily functionalized structures either at their *meso*, 2-, and 6-positions or through methylene substitution by styryl bridge derivatives.[12] We hypothesized that functionalization at the styryl position can result in interesting calix[4]-arene-based chemosensors, as it was previously described with calix[4]pyrrole derivatives.[27,28] This strategy requires us to functionalize the calix[4]arene scaffold with an aldehyde group. This selective functionalization can be easily achieved by controlling the electron-donating or -withdrawing character of calixarene phenols, which strongly determine the active positions toward electrophilic aromatic substitution.[29]

Mono(calix[4]arene)-substituted BODIPY probe **1** was prepared by Knoevenagel condensation of BODIPY **3** with 5-formyl-25,26,27,28-tetra-hydroxy-calix[4]arene **4** (Scheme 1).[28] Furthermore, for comparison purposes, the same condensation reaction was carried out with 4-hydroxybenzaldehyde **5** to synthesize dye **2**. Two different experimental conditions to perform this reaction were used. First, the conventional use of the Dean−Stark apparatus is using toluene as the solvent and *p*-toluenesulfonic acid/piperidine as catalysts. In this procedure, to achieve high conversion rates, temperature has to be rather harsh (reflux at 140−160 °C for 12 h), which generates many impurities and makes further purification difficult. As an alternative, a recent protocol using DMF as the solvent allowed for easier purification, mainly because of the use of milder conditions (reflux at 130 °C for 2 h).[30]

2.2. Photophysical Properties. As is known, the photophysical property changes of BODIPY derivatives are highly dependent on the employed solvent. For this reason, absorption and emission spectra of compounds **1** and **2** were registered in $CHCl_3$ and DMSO (10 μM, λ_{exc} = 540 nm). The corresponding normalized UV−vis spectra of 10 μM solutions are shown in Figure 1 and summarized in Table 1.

In the case of chloroform, **1** and **2** exhibit similar absorption spectra. Both molecules show a strong absorption band centered at 577 nm with a shoulder at 540 and 539 nm, respectively. As it has been previously discussed in the literature, the band at 577 nm corresponds to a S_0-S_1 transition, while the shoulder around 540 nm corresponds to a vibrational band of the S1 absorption.[31] The similarity between these spectra and those reported in the literature for some related compounds[32] suggests that the main absorption feature of **1** is arising from the extension of the π-system through the styryl linkage of BODIPY with a phenolic group.

In the case of DMSO, a different absorption profile is observed between **1** and **2**. The reference compound **2** exhibits two bands centered at 578 and 542 nm, similar to those observed in chloroform, whereas compound **1** shows the same band at 580 nm and a new band at 620 nm, which overlaps with the former. This strong difference in absorption also enlightens the crucial role that calix[4]arene plays in the absorption properties of **1** in DMSO. The appearance of the band at 620 nm could be related to the formation of a J-dimer that usually induces a strong bathochromic shift of the absorption band.[33,34] The J-dimer formation hypothesis was corroborated by the fluorescence behavior of both compounds

Scheme 1. Synthesis of Mono(calix[4]arene) Chemosensor 1 (25%) and Dye 2 (17%)

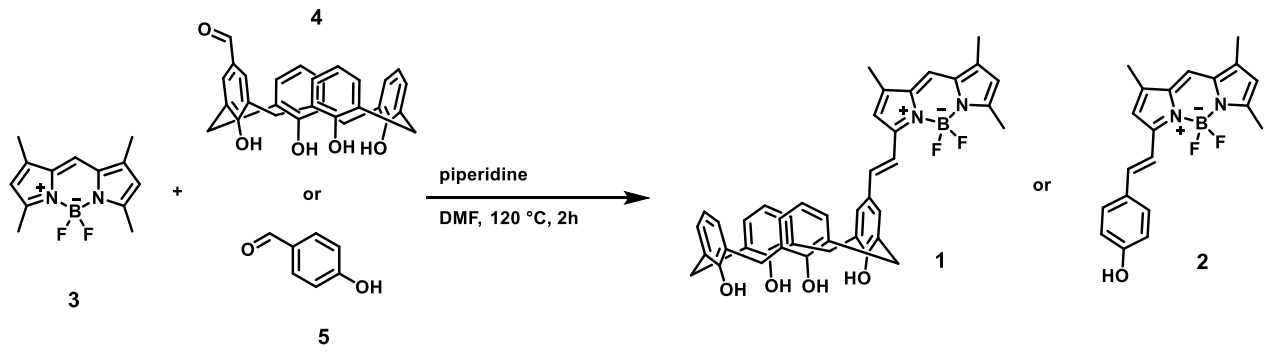

https://doi.org/10.1021/acsomega.2c06161
ACS Omega 2023, 8, 819−828

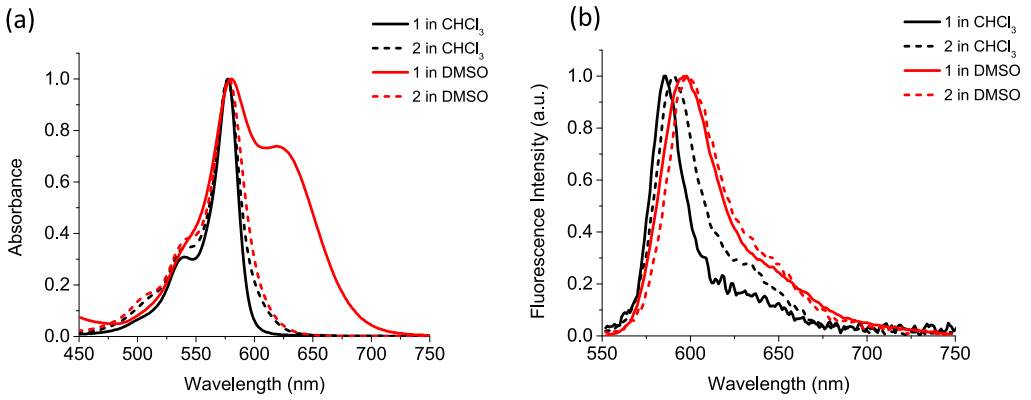

Figure 1. Normalized (a) absorption and (b) emission spectra (λ_{exc} = 540 nm) from **1** and **2** in $CHCl_3$ and DMSO solutions (10 μM).

Table 1. Absorption and Emission Bands of 1 and 2 in $CHCl_3$ and DMSO (10 μM)

	UV−vis		emission[a]	
compound	λ_{max} in $CHCl_3$ (nm)	λ_{max} in DMSO (nm)	λ_{max} in $CHCl_3$ (nm)[b]	λ_{max} in DMSO (nm)[b]
1	577; 540	580; 620	586	596
2	577; 539	578; 542	591	598

[a] λ_{exc} = 540 nm. [b] λ_{em} of the monomeric species.

in the studied solvents. Thus, the fluorescence spectra of compounds **1** and **2** in $CHCl_3$ show similar emission profiles when excited at 540 nm, with a maximum emission band at 586 and 591 nm, respectively, and similar intensities for both compounds (specifically, the quantum yield for compound **1** was 0.94). By contrast, a different behavior was observed when the compounds were dissolved in DMSO. Both compounds show a slight bathochromic shift of the emission bands that appear at 596 and 598 nm for **1** and **2**, respectively. This small shift in the emission maximum upon solvent change might be attributed to the different polarity of the solvent, which increases wavelength emission due to the stabilization of the excited state.[35] However, the stronger differences between both compounds are related to the emission intensity. Thus, although compound **2** shows in DMSO a similar emission intensity to that in $CHCl_3$, the fluorescence emission of the solution of **1** in DMSO diminishes with time, and after 24 h, a clear quenching of fluorescence is observed. The quantum yield measured for the solution of **1** in DMSO was 0.03. These results agree with a slow formation of J-aggregates.[36]

On the other hand, during characterization of the spectroscopic properties of **1** in DMSO, an unexpected behavior was observed. The relation within the absorption bands at 580 and 620 nm changed when the solution was prepared in volumetric glass and quartz cuvettes or stored in conventional glass vials. Simultaneously, the fluorescence emission was also affected, showing a remarkable decrease in the latter case. We were able to reproduce and control these changes by adding a small amount of SiO_2 (0.1 wt %) to the solutions prepared in volumetric glass or quartz cuvettes (Figure 2). The observed changes were the same as those previously observed in this solvent, but they took place faster. This anomalous behavior could also be related to aggregate formation because it has been described that this process can be promoted by the adsorption of monomers onto silica surfaces.[37]

2.3. NMR Studies. To understand the significant solvatochromic effect observed in compound **1** when the solvent changes from $CHCl_3$ to DMSO, NMR studies were carried out in both solvents. The spectra registered indicate that the calixarene moiety presents a symmetrical geometry due to the set of aromatic signals that appear in both spectra. This fact suggests a cone or a 1,3-alternated conformation. Additionally, a strong downfield shift of the signals corresponding to the hydrogens of the BODIPY moiety (see Table 2 and Figure 3) was observed in DMSO. Since this effect was observed not only in compound **1** but also in **2**, it means that it is not due to the presence of the calixarene moiety but the BODIPY core. Following the hypothesis about the formation of a dimer in DMSO, the influence of the

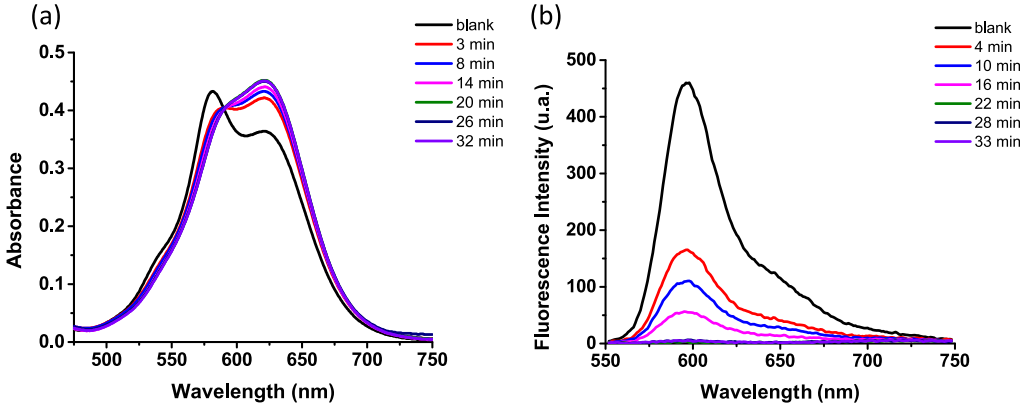

Figure 2. (a) Changes in UV−vis and (b) fluorescence spectra upon addition of SiO_2 (0.1 wt %) to a solution (10 μM) of **1** in DMSO.

https://doi.org/10.1021/acsomega.2c06161
ACS Omega 2023, 8, 819−828

Table 2. Comparison of the Chemical Shifts of the Protons of 1 in $CDCl_3$ and in DMSO-d_6

δ (ppm)	H_a	H_b	H_c	H_d	H_e	H_f	H_g	H_h	H_i	H_j	H_k	H_l
$CDCl_3$	6.99	6.59	6.07	4.26	3.58	7.36	7.08	7.27	6.77	7.04	6.72	7.13
DMSO	7.58	6.89	6.21	3.93	3.89	7.16	7.36	7.35	6.65	7.10	6.63	7.10

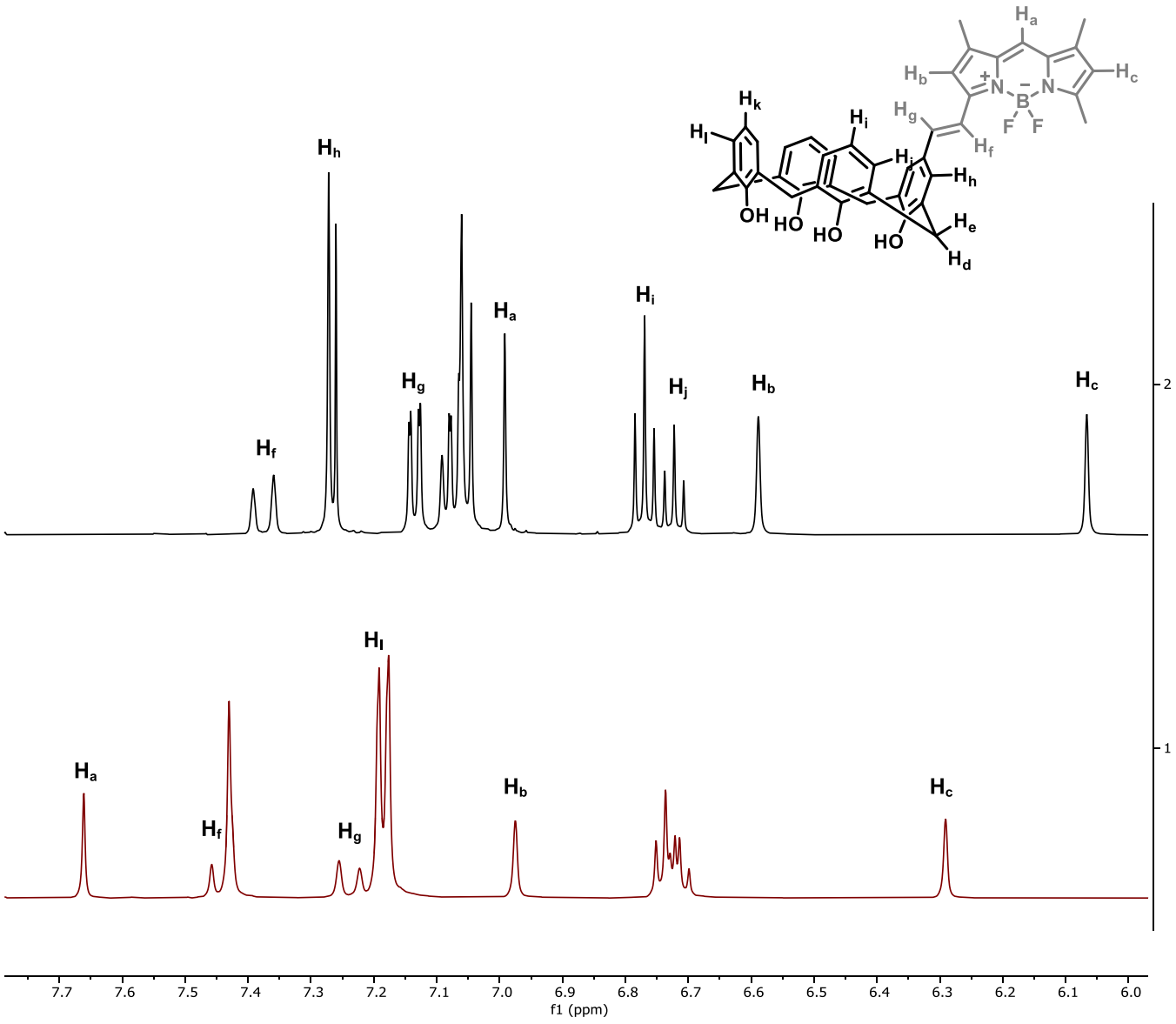

Figure 3. ^{1}H NMR (aromatic zone) comparison of 1 in $CDCl_3$ (top) and in DMSO-d_6 (bottom).

concentration on the chemical shifts of the BODIPY hydrogen signals was evaluated. Thus, ^{1}H NMR spectra at 10^{-2}, 10^{-3}, and 10^{-4} M concentrations were registered. As the concentration decreased, the signal corresponding to H_a was up-field shifted from 7.58 to 7.49 ppm, and proton H_c was also up-shifted from 6.21 to 6.16 ppm, whereas H_b remained unaffected (see Figure S12 in the Supporting Information). These modifications are in line with the hypothesis of a decrease in dimer concentration and a concomitant increase in the monomer concentration at low calixarene derivative concentrations.

Finally, a NOESY experiment was carried out in $CDCl_3$ and in DMSO-d_6. In $CDCl_3$, no unexpected NOE peaks were observed. However, in DMSO-d_6, strong NOEs between H_a and H_f and between H_a and H_h appeared in the spectrum. These signals can only be understood if some aggregation places two BODIPY moieties close to each other. Such a proposal is depicted in Figures 4 and S11.

The proposed dimer structure does not only justify the observed NOEs but also the substantial downfield shift of H_b as it is placed in the zone of influence of the field generated by the styrene double bond.

2.4. Cation Detection. The spectroscopic properties of SiO_2-treated DMSO solution (**1OP**) encouraged us to consider its application as a colorimetric and "OFF−ON" fluorescent probe for the detection of metal cations. The proposed mechanism was that the formation of a strong complex between the monomer and the cation could induce a disaggregation process with the corresponding color change and fluorescence enhancement. The spectroscopic changes of

https://doi.org/10.1021/acsomega.2c06161
ACS Omega 2023, 8, 819−828

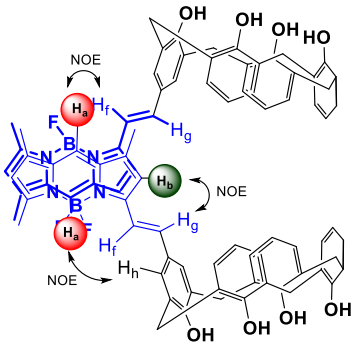

Figure 4. Proposed dimer structure.

1OP were studied upon addition of alkaline, alkaline-earth, and transition metals (Ag^{+}, K^{+}, Cs^{+}, Ca^{2+}, Ba^{2+}, Mg^{2+}, Zn^{2+}, Pb^{2+}, Fe^{2+}, Cu^{2+}, Hg^{2+}, Al^{3+}, Cr^{3+}, and Fe^{3+}) as nitrate or perchlorate salts. The screening experiments were carried out by adding 5 equiv of each cation (Figures 5 and S13 left).

The colorimetric changes of **1OP** upon adding the cations consist of a decrease in the band intensity at 620 nm and an increase in a new band at 580 nm. This behavior allowed us to evaluate ratiometrically the response of **1OP**, revealing that Hg^{2+} was the cation that gave rise to a significant colorimetric response (Figure 5a), allowing its "naked-eye" detection (see Figure S15).

Similarly, when studying the fluorescent response of **1OP** at an excitation wavelength of 540 nm, only Hg^{2+}, Al^{3+}, and Fe^{3+} gave a significant response (Figures 5b and S13 right), with Hg^{2+} being the most relevant cation for the application of **1OP** as a fluorescent chemosensor.

Colorimetric and fluorescent interference studies, in which an equimolar amount of Hg^{2+} was added to a solution of **1OP** with the corresponding cation, show that the binding to Hg^{2+} is dominant (Figure S14).

2.5. Titrations. Having assessed the selective response of **1OP** toward Hg^{2+}, the sensitivity of the probe was studied by monitoring the changes in UV−vis and fluorescence emission spectra of DMSO solutions upon addition of increasing quantities of the cation. The UV−vis profile is shown in Figure 6. As observed, after adding Hg^{2+}, a decrease in the visible band at 620 nm was registered, together with the simultaneous increase of a new band at 580 nm with an evident isosbestic point at 590 nm.

On the other hand, upon excitation of the sample at 540 nm, intense emission was observed at 598 nm, which increased with the addition of Hg^{2+}.

From the UV−vis and fluorescence titrations, the limits of detection (LoDs) of **1OP** were estimated by using the regression approach from IUPAC (Figures S16 and S17). The obtained values were 0.82 and 1.34 μM, respectively (Table 2).

Apparent association constants for **1OP·Hg^{2+}** were estimated by linear fitting, according to the Hill equation, with log K_{app} being 4.65 and 5.48, respectively (Table 3 and Figure S18).[38] The estimated Hill coefficients were n = 1.14 for both absorption and fluorescence titrations.

To gain some insight into the coordination mode and identify the changes on which it depends, ^{1}H NMR titration studies of **1** with Hg^{2+} in DMSO-d_6 were carried out. The most remarkable information was obtained from the signals related to the methylene bridges, which indicated that the conformation of calixarene was maintained in the range of 0 to 5 equiv (Figures 7 and S19). When the changes in the aromatic region were considered, it could be concluded that they were similar to those observed in the dilution experiments. However, in this case, H_a also showed a clear up-field shift. These facts, as well as the fluorescence recovery after complexation, suggested that the BODIPY moiety was involved to some extent in the disaggregation process and in the formation of a 1:1 complex with Hg^{2+}.

2.6. Theoretical Calculations. *2.6.1. Molecular Geometries and Spectral Features.* In order to shed light on the interesting spectroscopic properties of compound **1**, a series of theoretical calculations were carried out. Thus, a conformational analysis as well as a stability study of possible aggregates were done.

2.6.2. Conformational Analysis of 1. The four typical conformers of the calix[4]arene unit of **1** were found (see Scheme 2) and confirmed as minima on the potential energy surface at the IEFPCM/B3LYP-D3/Def2SVP level, employing $CHCl_3$ and DMSO as solvents. As can be seen in Table 4, both the Gibbs free energy and electronic energy revealed that cone conformation was predicted as the most stable one in both solvents. Additionally, these results indicated that **1** existed

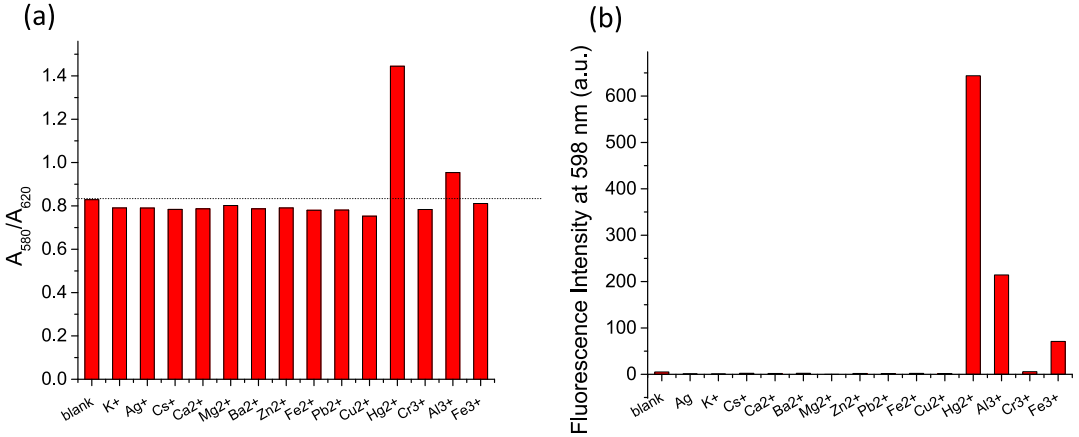

Figure 5. (a) Ratiometric absorption changes of **1OP** (A_{580}/A_{620}). (b) Fluorescence increase at 598 nm upon addition of 5 equiv of each metal in DMSO solutions (10 μM).

https://doi.org/10.1021/acsomega.2c06161
ACS Omega 2023, 8, 819−828

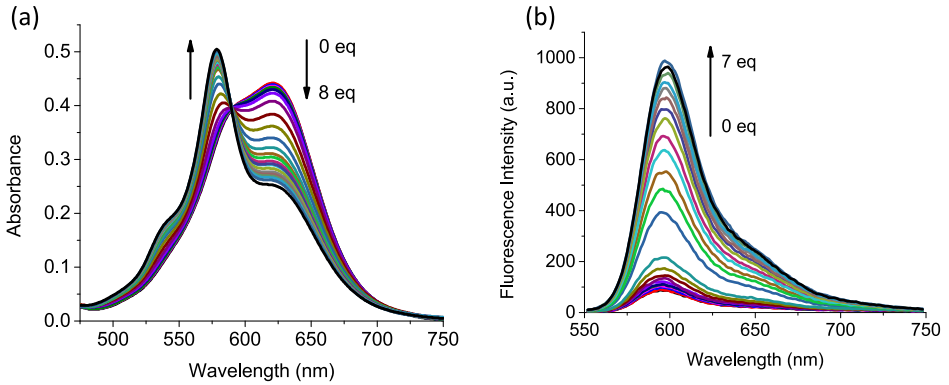

Figure 6. (a) Absorption and (b) emission titration curves for **1OP** (10 μM in DMSO, λ_{exc} = 540 nm).

Table 3. Log K_{app}, Hill Coefficient, and LOD of UV−vis, and Fluorescence Titrations of 1OP with Hg^{2+} in DMSO

method	log K_{app}	n	LoD (μM)
UV−vis	4.65	1.14	0.82
fluorescence	5.48	1.14	1.34

totally in the cone conformation in solution, according to Boltzmann distribution at room temperature.

2.6.3. Aggregate Types of 1. In the present study, two types of dimers were found in both solvents and confirmed as minima on the potential energy surface as displayed in Scheme 3. These were labeled as cisoid (a) or transoid (b), depending on the relative position of the calixarene moiety. In both types of dimers, the BODIPY moieties were stacked antiparallel to each other. While both isomeric dimers were quite isoenergetic in $CHCl_3$, the cisoid one was more stable than the transoid in DMSO by 0.77 kcal/mol. Gibbs free binding energy together with the Boltzmann population of both aggregate types are quoted in Table 5.

At first glance, our calculations unveiled that the binding process of both aggregate types was exergonic in both solvents but slightly more in $CHCl_3$ than in DMSO. In addition, cisoid/transoid populations would be similar in $CHCl_3$ (52:48%) but not in DMSO (79:21%; see Table 5) under thermodynamic control. However, experimental observations indicate that in chloroform solutions, the main product was the monomer, whereas in DMSO, it was the dimer. These data suggested a kinetic control of the dimerization process (Figure 8).

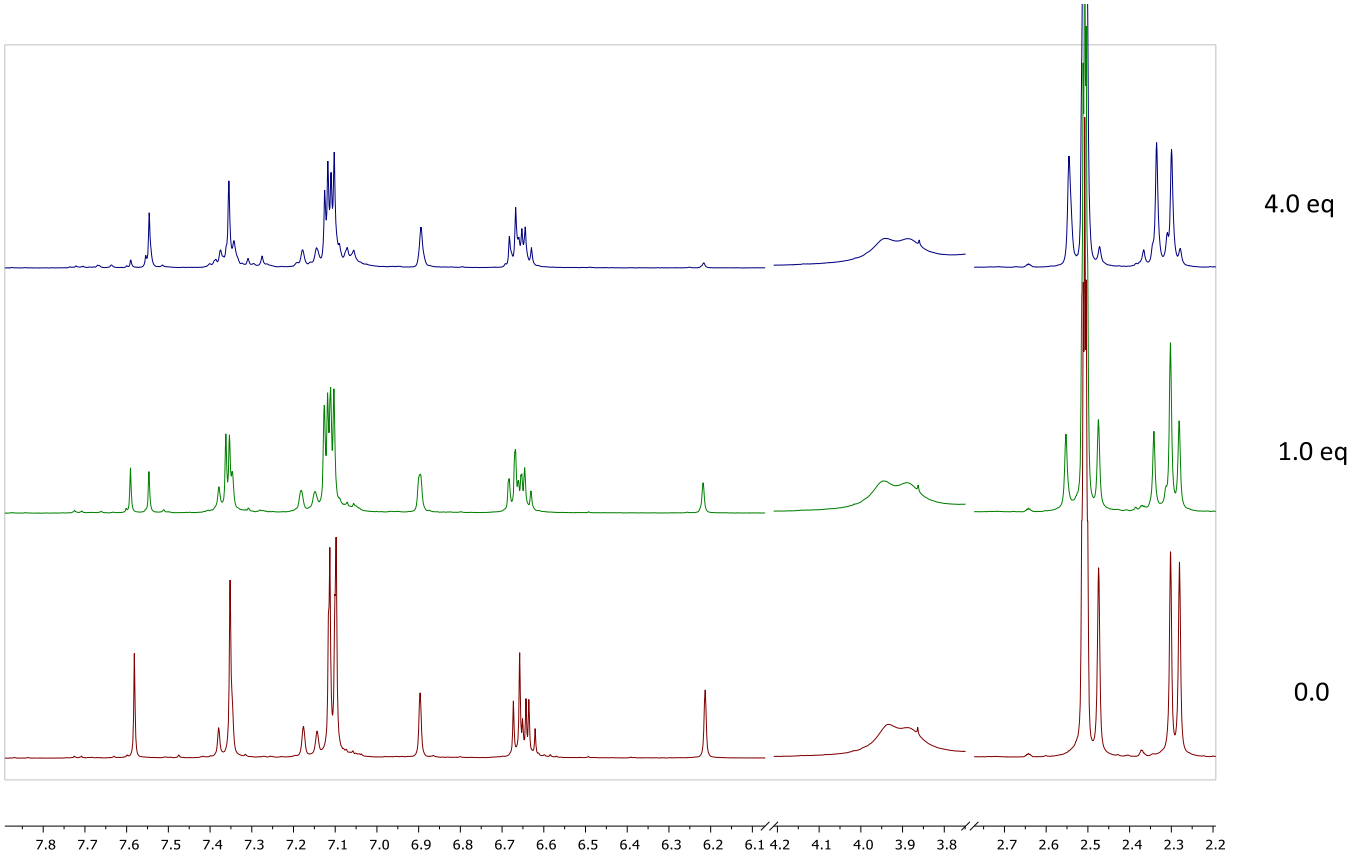

Figure 7. ^{1}H NMR study of **1** in DMSO-d_6 upon increasing amounts of Hg^{2+}.

https://doi.org/10.1021/acsomega.2c06161
ACS Omega 2023, 8, 819−828

Scheme 2. Studied Conformations of 1 in DMSO and in $CHCl_3$

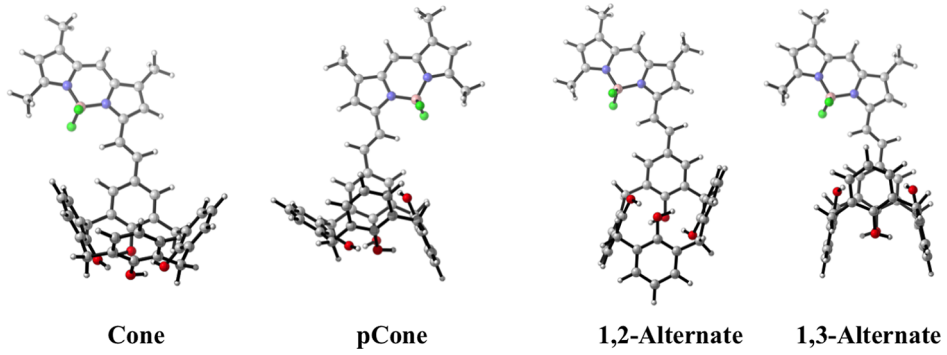

Table 4. Relative Gibbs Free Energies and Relative Electronic Energies (in Brackets) Computed for the Studied Conformations of 1 at IEFPCM/B3LYP-D3/Def2SVP Level[a]

conformer	relative Gibbs free energy in $CHCl_3$	relative Gibbs free energy in DMSO
cone	0.00 [0.00]	0.00 [0.00]
pCone	7.62 [8.73]	7.22 [8.72]
1,2-alternate	9.95 [11.64]	9.42 [11.51]
1,3-alternate	12.78 [14.88]	11.96 [14.93]

[a]All data are in kcal/mol.

Scheme 3. Types of Dimers of 1, (a) Cisoid, and (b) Transoid-Type

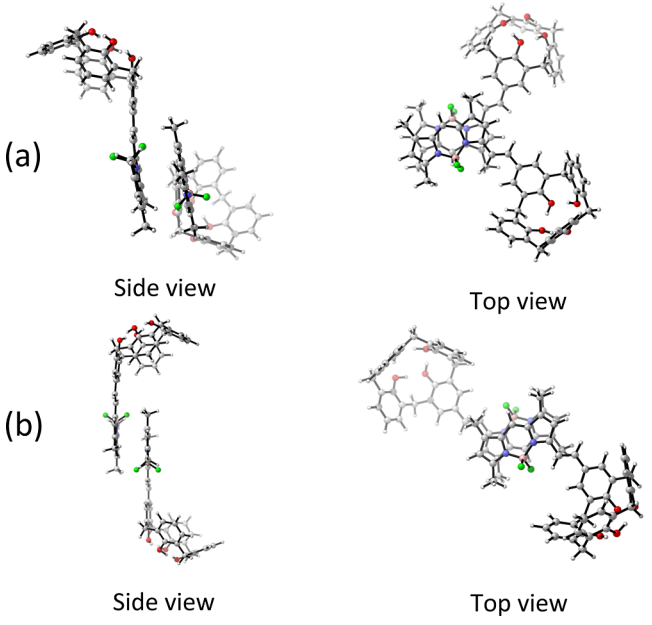

Table 5. Gibbs Free Binding Energy (in kcal/mol) and Boltzmann's Population (in Brackets) Computed at IEFPCM/B3LYP-D3/Def2SVP for the Isomeric Dimers

aggregate	Gibbs free binding energy in $CHCl_3$	Gibbs free binding energy in DMSO
cisoid	−6.25 [52%]	−5.66 [79%]
transoid	−6.21 [48%]	−4.89 [21%]

As it has been indicated above, the fluorescence properties of the monomeric sensor in DMSO were recovered as the dimer

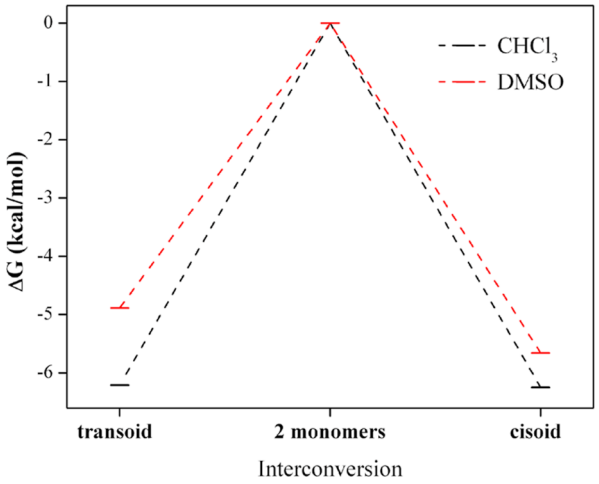

Figure 8. Gibbs free energy profile for the transoid and cisoid dimers and the monomer in both studied solvents.

interacted with Hg^{2+}. Accordingly, our calculations revealed an intercalation-type complex that interrupted the intermolecular interactions of the stacked BODIPY units (see Scheme 4a), with 7.25 kcal/mol being more stable. In turn, this complex was capable of evolving toward an even more stable complex with a stoichiometry of 1:1 and with an interaction energy of −10.68 kcal/mol (see Scheme 4b) that would explain the ON mode of the chemosensor since its spectral features were quite similar to those of the free monomer, but with a lower oscillator strength.

3. CONCLUSIONS

The calixarene-BODIPY derivative **1** has shown interesting changes in its photophysical properties depending on the solvent. In this regard, the typical absorption and emission bands of the BODIPY moiety are observed in chloroform, whereas a new absorption band, along with the quenching of fluorescence, is observed in DMSO. NMR dilution studies on both solvents revealed that this behavior may be related to its possible dimerization. From the calixarene point of view, NMR spectra indicate that, in both monomer and dimer forms, it adopts a symmetrical conformation. Modelization at the IEFPCM/B3LYP-D3/Def2SVP level confirms both the major stability of cone conformation in the monomer and the stability of J-dimer-type formation in both solvents. Two dimers, cisoid and transoid, emerge as the most stable ones, with a theoretical proportion of 52:48 in $CHCl_3$ and 79:21 in DMSO. The higher stability of the dimer versus the monomer

https://doi.org/10.1021/acsomega.2c06161
ACS Omega 2023, 8, 819−828

Scheme 4. Binding Modes between (a) Hg^{2+} and Cisoid Dimers (Interaction Energy is −7.25 kcal/mol) and (b) Hg^{2+} and Cone Monomers (the Interaction Energy is −10.68 kcal/mol)

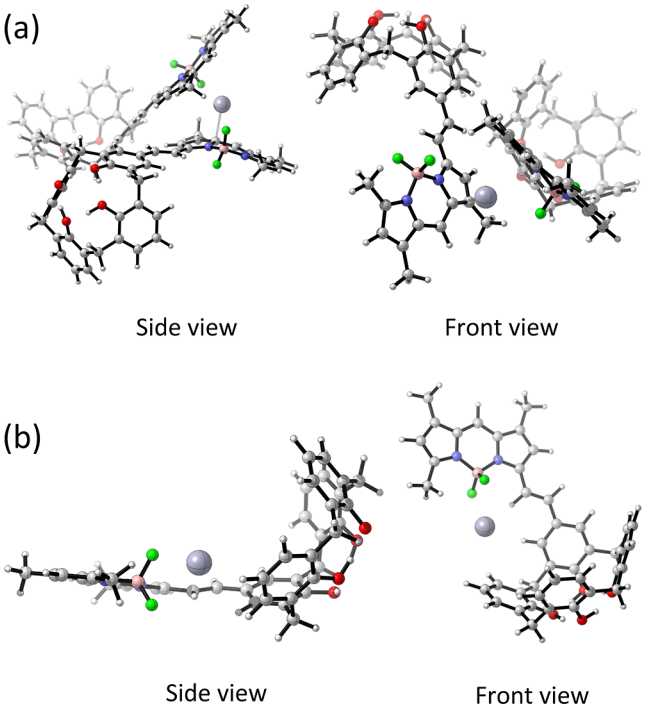

in $CHCl_3$ contrasts with the ^1H NMR spectra, which is similar to the spectra of highly diluted samples. However, the high concentration of the monomer in $CHCl_3$ may be due to a kinetic control, with a bigger barrier in $CHCl_3$ than in DMSO. We have observed that, even in DMSO, a small amount of SiO_2 is required to catalyze the formation of dimers with the concomitant disappearance of its fluorescence. NMR spectra, at higher concentrations, are consistent with the generation of dimers in DMSO, but in $CDCl_3$ monomers, they still predominate.

The addition of different cations to non-fluorescent DMSO solutions led to a strong increase in the fluorescence intensity only in the case of Hg^{2+} both alone and in the presence of other metal cations. Molecular modeling studies show that the breakdown of the dimer due to the intercalation of the Hg^{2+} cation between the two BODIPY structures, breaking their $\pi-\pi$ interaction, is responsible for fluorescence recovery. Therefore, it can be ascertained that mono(calix[4]arene)-substituted BODIPY dye **1** is a mercury-selective fluorogenic sensor with an unconventional OFF−ON detection mechanism based on dimer formation/breakage.

4. MATERIALS AND METHODS

The reagents employed in the synthesis were acquired from Sigma-Aldrich and used without further purification. The solvents used were dried and distilled under argon prior to use. Silica gel 60 F254 (Merck) plates were used for TLC. Column chromatography was performed on silica gel.

For screening assays and tritiations, either the perchlorate or nitrate salts of the cations K^+, Cs^+, Ba^{2+}, Mg^{2+}, Ca^{2+}, Ag^+, Zn^{2+}, Pb^{2+}, Cu^{2+}, Fe^{2+}, Hg^{2+}, Al^{3+}, Cr^{3+}, and Fe^{3+} are used. No effect of the counterions was observed during the experiments. Stock solutions of 10^{-3} M of **1** and the cations were prepared, and dilution to 10^{-5} M was prepared in the cuvette. For interference studies, 5 equiv of each cation were added to a solution 10^{-5} M of the probe; afterward, 5 equiv of Hg^{2+} were also added.

Absolute photoluminescence quantum yields (ΦPL) were recorded using an integrating sphere system with a reflectance higher than 99% in the range of 400−1500 nm on a FLS1000 photoluminescence spectrometer (Edinburgh Instruments). For reference, a neat solvent with exactly the same volume was used. All spectra were recorded using a 1 cm path-length quartz cuvette at room temperature.

^1H, ^{13}C NMR, COSY, HSQC, and NOESY spectra were determined with Bruker Avance 300 and 500 MHz spectrometers. Chemical shifts are reported in parts per million (ppm) and referenced to the solvent peak. High-resolution mass spectra were recorded in the positive ion mode with a TripleTOF 5600 LC/MS/MS System AB SCIEX mass spectrometer. All photophysical analyses were carried out in air-equilibrated DMSO or MeCN at 298 K. Absorption spectra were recorded with a Shimadzu UV-2600 spectrophotometer. Fluorescence spectra were carried out on a VarianCary Eclipse fluorimeter. Quartz cells with a path length of 1.0 cm were used. Origin 2020 was the program used to plot titrations and to calculate complexation constants.

5-Formyl-25,26,27,28-tetra-hydroxy-calix[4]arene **4** and BODIPY **3** were synthesized by previously reported synthetic procedures.[8,29,39]

4.1. Synthesis. *4.1.1. Synthesis of* ***1****.* BODIPY **3** (155 mg, 0.63 mmol) and 5-formyl-25,26,27,28-tetra-hydroxy-calix[4]-arene **4** (142 mg, 0.31 mmol) were dissolved in DMF (4 mL). Afterward, piperidine (100 μL) was added, and the mixture was heated at 120 °C for 2 h. The mixture was cooled to room temperature before adding acidified water (HCl 0.1 M). The aqueous phase was extracted three times with dichloromethane, and the combined organic fractions were dried with $MgSO_4$. After filtration, the solvent was evaporated, and the crude was adsorbed into silica. Purification was realized using silica gel as the stationary phase and ethyl acetate/hexane mixtures as the eluent (1:9, 1:4, and 1:2, successively). The product was obtained as a violet solid (55 mg, 25%).

^1H NMR (500 MHz, chloroform-*d*): δ (ppm) 10.18 (s, 4H), 7.36 (d, *J* = 16.4 Hz, 1H), 7.27 (s, 2H), 7.13 (dd, *J* = 7.6, 1.6 Hz, 2H), 7.07 (m, 5H), 6.99 (s, 1H), 6.77 (t, *J* = 7.56 Hz, 2H), 6.72 (t, *J* = 7.56 Hz, 1H), 6.59 (s, 1H), 6.07 (s, 1H), 4.26 (br s, 4H), 3.58 (br s, 4H), 2.59 (s, 3H), 2.26 (s, 3H), 2.25 (s, 3H).

^1H NMR (500 MHz, DMSO-d_6): δ (ppm) 9.89 (br s, 4H), 7.58 (s, 1H), 7.36 (m, 3H), 7.15 (d, *J* = 16.3 Hz, 1H), 7.10 (m, 6H), 6.89 (s, 1H), 6.65 (t, *J* = 6.65 Hz, 2H), 6.63 (t, *J* = 7.54 Hz, 1H), 6.21 (s, 1H), 3.92 (br s, 4H), 3.88 (br s, 4H), 2.47 (s, 3H), 2.30 (s, 3H), 2.27 (s, 3H).

^{13}C NMR (125 MHz, chloroform-*d*): δ (ppm) 156.18; 154.63; 150.25; 148.86; 148.78; 140.67; 140.51; 136.35; 135.09; 133.84; 130.85; 129.33; 129.26; 129.13; 128.88; 128.55; 128.44; 128.27; 127.97; 122.57; 122.46; 119.08; 118.51; 117.46; 115.59; 32.08; 31.81; 31.78; 30.46; 30.19; 29.85; 29.51; 22.84; 14.96; 14.27; 11.46; 11.45.

HRMS: *m*/*z* calc for $C_{42}H_{41}BF_2N_3O_4$ (M + NH_4), 700.3153; found, 700.3139 $[M + NH_4]^+$.

4.1.2. Synthesis of ***2****.* Following the same procedure as in **1** (17%).

^1H NMR (300 MHz, chloroform-*d*): δ (ppm) 8.07 (s, 1H), 7.53−7.38 (m, 3H), 7.20 (d, *J* = 16.3 Hz, 1H), 7.01 (s, 1H),

https://doi.org/10.1021/acsomega.2c06161
ACS Omega 2023, 8, 819−828

6.83 (dd, J = 8.7, 2.3 Hz, 2H), 6.65 (s, 1H), 6.07 (s, 1H), 2.57 (s, 3H), 2.29 (s, 3H), 2.26 (s, 3H).

^{1}H NMR (300 MHz, DMSO-d_6): δ 9.96 (s, 1H), 7.59 (s, 1H), 7.49 (d, J = 16.4 Hz, 1H), 7.44 (d, J = 8.7 Hz,2), 7.22 (d, J = 16.3 Hz, 1H), 6.93 (s, 1H), 6.85 (d, J = 8.6 Hz, 2H), 6.20 (s, 1H), 2.45 (s, 1H), 2.31 (s, 1H), 2.28 (s, 1H).

■ ASSOCIATED CONTENT

Supporting Information

The Supporting Information is available free of charge at https://pubs.acs.org/doi/10.1021/acsomega.2c06161.

Materials and methods, synthesis, NMR spectra (^{1}H NMR, ^{13}C NMR, COSY, ^{13}C ^{1}H HSQC, and NOESY), studies with cations (screening, competitivity, and images under natural and 365 nm UV light), limits of detection, equilibrium constants, ^{1}H NMR titration, comparison with calixarene-based chemosensors, and computational details (PDF)

■ AUTHOR INFORMATION

Corresponding Authors

Alejandro Lorente − *Departamento de Química Orgánica y Fisicoquímica, Facultad de Ciencias Químicas y Farmacéuticas, Universidad de Chile, 8380492 Independencia, Santiago, Chile; Institut für Chemie und Biochemie, Freie Universität Berlin, 14195 Berlin, Germany;* orcid.org/0000-0002-3266-5336; Email: alorentesanchez@gmail.com, a.lorente.sanchez@fu-berlin.de

Pablo Jaque − *Departamento de Química Orgánica y Fisicoquímica, Facultad de Ciencias Químicas y Farmacéuticas, Universidad de Chile, 8380492 Independencia, Santiago, Chile;* orcid.org/0000-0002-4055-3553; Email: pablo.jaque@ciq.uchile.cl

José A. Sáez − *Instituto Interuniversitario de Investigación de Reconocimiento Molecular y Desarrollo Tecnológico, Universitat de València-Universitat Politècnica de València, 46100 Valencia, Spain; Departamento de Química Orgánica, Universidad de Valencia, 46100 Valencia, Spain;* Email: josesaez@uv.es

Authors

Andres Ochoa − *Departamento de Química Orgánica y Fisicoquímica, Facultad de Ciencias Químicas y Farmacéuticas, Universidad de Chile, 8380492 Independencia, Santiago, Chile*

Julio Rodriguez-Lavado − *Departamento de Química Orgánica y Fisicoquímica, Facultad de Ciencias Químicas y Farmacéuticas, Universidad de Chile, 8380492 Independencia, Santiago, Chile*

Silvia Rodriguez-Nuévalos − *Instituto Interuniversitario de Investigación de Reconocimiento Molecular y Desarrollo Tecnológico, Universitat de València-Universitat Politècnica de València, 46100 Valencia, Spain*

Salvador Gil − *Instituto Interuniversitario de Investigación de Reconocimiento Molecular y Desarrollo Tecnológico, Universitat de València-Universitat Politècnica de València, 46100 Valencia, Spain; Departamento de Química Orgánica, Universidad de Valencia, 46100 Valencia, Spain*

Ana M. Costero − *Instituto Interuniversitario de Investigación de Reconocimiento Molecular y Desarrollo Tecnológico, Universitat de València-Universitat Politècnica de València, 46100 Valencia, Spain; Departamento de Química Orgánica, Universidad de Valencia, 46100 Valencia, Spain;* orcid.org/0000-0001-9640-1148

Complete contact information is available at: https://pubs.acs.org/10.1021/acsomega.2c06161

Author Contributions

A.L.: investigation (design of chemosensors, synthesis, characterization, and cation interaction evaluation), conceptualization, and writing—original draft. A.O.: investigation (synthesis); J.R.-L.: investigation (synthesis); S.R.-N.: methodology and investigation; P.J.: theoretical calculations, conceptualization, and writing—original draft; S.G.: NMR studies and cation interaction evaluation; A.M.C: supervision, conceptualization, and writing—original draft; and J.A.S.: collaboration in theoretical interpretation and revision and editing of the manuscript.

Notes

The authors declare no competing financial interest.

■ ACKNOWLEDGMENTS

We gratefully acknowledge financial support from Fondecyt Postdoctoral Grants 3170264 and 3180041. PJ acknowledges Fondecyt project no 1181914. Grant RTI2018-100910-B-C42 was funded by MCIN/AEI/10.13039/501100011033 and by "ERDF - A way of making Europe". SCSIE (Universitat de València) is gratefully acknowledged for all the equipment employed. NMR was registered at the U26 facility of ICTS "NANBIOSIS" at the Universitat of València. Funding was also received through the Einstein Research Unit "Climate and Water under Change" from the Einstein Foundation Berlin and Berlin University Alliance (Grant ERU-2020-609). We also want to thank Natxo M. Hermoso (www.natxohermoso.com) for helping us with all the photography in this work.

■ REFERENCES

(1) Tchounwou, P. B.; Yedjou, C. G.; Patlolla, A. K.; Sutton, D. J. Heavy Metal Toxicity and the Environment. In *Molecular, Clinical and Environmental Toxicology*; Luch, A., Ed.; Springer Basel: Basel, 2012; Vol. *101*, pp 133−164.

(2) Schaider, L. A.; Senn, D. B.; Estes, E. R.; Brabander, D. J.; Shine, J. P. Sources and Fates of Heavy Metals in a Mining-Impacted Stream: Temporal Variability and the Role of Iron Oxides. *Sci. Total Environ.* **2014**, *490*, 456−466.

(3) Vandecasteele, C.; Cornelis, G. Oxyanions in Waste: Occurrence, Leaching, Stabilisation, Relation to Wastewater Treatment. In *Water Treatment Technologies for the Removal of High-Toxity Pollutants*; Václavíková, M., Vitale, K., Gallios, G. P., Ivaničová, L., Eds.; Springer Netherlands: Dordrecht, 2009; pp 149−159.

(4) Langford, N. J.; Ferner, R. E. Toxicity of Mercury. *J. Hum. Hypertens.* **1999**, *13*, 651−656.

(5) Bernhoft, R. A. Mercury Toxicity and Treatment: A Review of the Literature. *J. Environ. Public Health* **2012**, *2012*, 460508.

(6) Davidson, C. M. Methods for the Determination of Heavy Metals and Metalloids in Soils. In *Heavy Metals in Soils; Environmental Pollution*; Springer: Dordrecht, 2013; pp 97−140.

(7) Gotor, R.; Gaviña, P.; Costero, A. M. Low-Cost, Portable Open-Source Gas Monitoring Device Based on Chemosensory Technology. *Meas. Sci. Technol.* **2015**, *26*, 085103.

(8) Gotor, R.; Gaviña, P.; Ochando, L. E.; Chulvi, K.; Lorente, A.; Martínez-Máñez, R.; Costero, A. M. BODIPY dyes functionalized with 2-(2-dimethylaminophenyl)ethanol moieties as selective OFF-ON fluorescent chemodosimeters for the nerve agent mimics DCNP and DFP. *RSC Adv.* **2014**, *4*, 15975−15982.

(9) Gotor, R.; Ashokkumar, P.; Hecht, M.; Keil, K.; Rurack, K. Optical pH Sensor Covering the Range from pH 0-14 Compatible with Mobile-Device Readout and Based on a Set of Rationally Designed Indicator Dyes. *Anal. Chem.* **2017**, *89*, 8437−8444.
(10) Wu, D.; Sedgwick, A. C.; Akkaya, T.; Yoon, E. U.; James, J.; James, T. D. Fluorescent Chemosensors: The Past, Present and Future. *Chem. Soc. Rev.* **2017**, *46*, 7105−7123.
(11) Treibs, A.; Kreuzer, F.-H. Difluorboryl-Komplexe von Di- und Tripyrrylmethenen. *Justus Liebigs Ann. Chem.* **1968**, *718*, 208−223.
(12) Ulrich, G.; Ziessel, R.; Harriman, A. The Chemistry of Fluorescent Bodipy Dyes: Versatility Unsurpassed. *Angew. Chem., Int. Ed.* **2008**, *47*, 1184−1201.
(13) Loudet, A.; Burgess, K. BODIPY Dyes and Their Derivatives: Syntheses and Spectroscopic Properties. *Chem. Rev.* **2007**, *107*, 4891−4932.
(14) Kim, D.; Yamamoto, K.; Ahn, K. H. A BODIPY-Based Reactive Probe for Ratiometric Fluorescence Sensing of Mercury Ions. *Tetrahedron* **2012**, *68*, 5279−5282.
(15) Sulak, M.; Kursunlu, A. N.; Girgin, B.; Karakuş, Ö. Ö.; Güler, E. A Highly Selective Fluorescent Sensor for Mercury (II) Ion Based on Bodipy and Calix[4]Arene Bearing Triazolenaphthylene Groups; Synthesis and Photophysical Investigations. *J. Photochem. Photobiol., A* **2017**, *349*, 129−137.
(16) Xue, Z.; Liu, T.; Liu, H. Naked-Eye Chromogenic and Fluorogenic Chemosensor for Mercury (II) Ion Based on Substituted Distyryl BODIPY Complex. *Dyes Pigm.* **2019**, *165*, 65−70.
(17) Rambo, B. M.; Kim, S. K.; Kim, J. S.; Bielawski, C. W.; Sessler, J. L. A Benzocrown-6-Calix[4]Arene Methacrylate Copolymer: Selective Extraction of Caesium Ions from a Multi-Component System. *Chem. Sci.* **2010**, *1*, 716−722.
(18) Santoyo-González, F.; Torres-Pinedo, A.; Barria, C. S. An Efficient Synthesis of Bis(Calix[4]Arenes), Bis(Crown Ether)-Substituted Calix[4]Arenes, Aza-Crown Calix[4]Arenes, and Thiaza-Crown Calix[4]Arenes. *Eur. J. Org. Chem.* **2000**, 3587−3593.
(19) Gutsche, C. D.; Lin, L.-G. Calixarenes 12. *Tetrahedron* **1986**, *42*, 1633−1640.
(20) Quiroga-Campano, C.; Gómez-Machuca, H.; Jullian, C.; la Fuente, J. D.; Pessoa-Mahana, H.; Saitz, C. Study by Fluorescence of Calix[4]Arenes Bearing Heterocycles with Divalent Metals: Highly Selective Detection of Pb2+. *J. Inclusion Phenom. Macrocycl. Chem.* **2014**, *79*, 161−169.
(21) Jose, P.; Menon, S. Lower-Rim Substituted Calixarenes and Their Applications. *Bioinorg. Chem. Appl.* **2007**, *2007*, 65815.
(22) Maher, N. J.; Diao, H.; O'Sullivan, J.; Fadda, E.; Heaney, F.; McGinley, J. Lower Rim Isoxazole-Calix[4]Arene Derivatives as Fluorescence Sensors for Copper(II) Ions. *Tetrahedron* **2015**, *71*, 9223−9233.
(23) Kim, H. J.; Kim, J. S. BODIPY Appended Cone-Calix[4]Arene: Selective Fluorescence Changes upon Ca2+ Binding. *Tetrahedron Lett.* **2006**, *47*, 7051−7055.
(24) Baki, C. N.; Akkaya, E. U. Boradiazaindacene-Appended Calix[4]Arene: Fluorescence Sensing of PH Near Neutrality. *J. Org. Chem.* **2001**, *66*, 1512−1513.
(25) Rodríguez-Lavado, J.; Lorente, A.; Flores, E.; Ochoa, A.; Godoy, F.; Jaque, P.; Saitz, C. Elucidating Sensing Mechanisms of a Pyrene Excimer-Based Calix[4]Arene for Ratiometric Detection of Hg(II) and Ag(I) and Chemosensor Behavior as INHIBITION or IMPLICATION Logic Gates. *RSC Adv.* **2020**, *10*, 21963−21973.
(26) Descalzo, A. B.; Ashokkumar, P.; Shen, Z.; Rurack, K. BehaviorOn the Aggregation Behavior and Spectroscopic Properties of Alkylated and Annelated Boron-Dipyrromethene (BODIPY) Dyes in Aqueous Solution. *ChemPhotoChem* **2020**, *4*, 120−131.
(27) Gotor, R.; Costero, A. M.; Gil, S.; Parra, M.; Gaviña, P.; Rurack, K. Boolean Operations Mediated by an Ion-Pair Receptor of a Multi-Readout Molecular Logic Gate. *Chem. Commun.* **2013**, *49*, 11056−11058.
(28) Gotor, R.; Costero, A. M.; Gil, S.; Gaviña, P.; Rurack, K. On the Ion-Pair Recognition and Indication Features of a Fluorescent Heteroditopic Host Based on a BODIPY Core. *Eur. J. Org. Chem.* **2014**, 4005−4013.
(29) Romero, P. E.; Piers, W. E.; Decker, S. A.; Chau, D.; Woo, T. K.; Parvez, M. η1 versus η5 Bonding Modes in Cp*Al(I) Adducts of 9-Borafluorenes. *Organometallics* **2003**, *22*, 1266−1274.
(30) Kang, H.; Si, Y.; Liu, Y.; Zhang, X.; Zhang, W.; Zhao, Y.; Yang, B.; Liu, Y.; Liu, Z. Photophysical/Chemistry Properties of Distyryl-BODIPY Derivatives: An Experimental and Density Functional Theoretical Study. *J. Phys. Chem. A* **2018**, *122*, 5574−5579.
(31) Zhao, Y.; Lv, X.; Liu, Y.; Liu, J.; Zhang, Y.; Shi, H.; Guo, W. The emission enhancement of the NIR distyryl Bodipy dyes by the indirect S0 → S2 excitation and their application towards a Hg2+ probe. *J. Mater. Chem.* **2012**, *22*, 11475−11478.
(32) Shao, J.; Guo, H.; Ji, S.; Zhao, J. Styryl-BODIPY based red-emitting fluorescent OFF-ON molecular probe for specific detection of cysteine. *Biosens. Bioelectron.* **2011**, *26*, 3012−3017.
(33) Zhang, Y.; Liu, P.; Pan, H.; Dai, H.; Ren, X.-K.; Chen, Z. Alignment of Supramolecular J-Aggregates Based on Uracil-Functionalized BODIPY Dye for Polarized Photoluminescence. *Chem. Commun.* **2020**, *56*, 12069−12072.
(34) Zhang, Y.; Yuan, S.; Liu, P.; Jing, L.; Pan, H.; Ren, X.-K.; Chen, Z. J-Aggregation Induced Emission Enhancement of BODIPY Dyes via H-Bonding Directed Supramolecular Polymerization: The Importance of Substituents at Boron. *Org. Chem. Front.* **2021**, *8*, 4078−4085.
(35) Cunha Dias de Rezende, L.; Menezes Vaidergorn, M.; Biazzotto Moraes, J. C.; da Silva Emery, F. Synthesis, Photophysical Properties and Solvatochromism of Meso-Substituted Tetramethyl BODIPY Dyes. *J. Fluoresc.* **2014**, *24*, 257−266.
(36) Guo, X.; Li, M.; Wu, H.; Sheng, W.; Feng, Y.; Yu, C.; Jiao, L.; Hao, E. Near-IR Absorbing J-Aggregates of a Phenanthrene-Fused BODIPY as a Highly Efficient Photothermal Nanoagent. *Chem. Commun.* **2020**, *56*, 14709−14712.
(37) Tleugabulova, D.; Zhang, Z.; Brennan, J. D. Characterization of Bodipy Dimers Formed in a Molecularly Confined Environment. *J. Phys. Chem. B* **2002**, *106*, 13133−13138.
(38) Santos-Figueroa, L. E.; Llopis-Lorente, A.; Royo, S.; Sancenón, F.; Martínez-Máñez, R.; Costero, A. M.; Gil, S.; Parra, M. A Chalcone-Based Highly Selective and Sensitive Chromofluorogenic Probe for Trivalent Metal Cations. *ChemPlusChem* **2015**, *80*, 800−804.
(39) Beatty, M. A.; Borges-González, J.; Sinclair, N. J.; Pye, A. T.; Hof, F. Analyte-Driven Disassembly and Turn-On Fluorescent Sensing in Competitive Biological Media. *J. Am. Chem. Soc.* **2018**, *140*, 3500−3504.

https://doi.org/10.1021/acsomega.2c06161
ACS Omega 2023, 8, 819−828